6th International Conference on Advances in Experimental Structural Engineering
11th International Workshop on Advanced Smart Materials and Smart Structures Technology
August 1-2, 2015, University of Illinois, Urbana-Champaign, United States

A Monitoring Method of M-ϕ Curve in Plastic Hinge Zone of the RC Structure

H.B. Zhang[1], S. Hou[2], J.P. Ou[3]

1 *Doctoral candidate, School of Civil Engineering, Dalian University of Technology, Dalian, China.*
E-mail: zhanghb01@gmail.com
2 *Associate professor, School of Civil & Transportation Engineering, South China University of Technology, Guangzhou, China.*
E-mail: CTHous@scut.edu.cn.
3 *Professor, School of Civil Engineering, Dalian University of Technology, Dalian, China.*
E-mail: oujinping@dlut.edu.cn.

ABSTRACT
Numerical simulation method is a good tool to evaluate the structure performance under extreme loading conditions such as earthquakes or blasts without great financial input on destruction tests. However, great difficulties still exist in accurate simulation of the nonlinear behaviour of large structures due to the uncertainty of constitutive parameter of the composed material. To overcome this problem, a measured data-based M-ϕ constitutive monitoring method is proposed in this paper for simulating the seismic response of RC building structures. The essential idea of the proposed method is that instrumenting the plastic hinge zone of RC structure with damage monitoring sensors: Smart aggregates were used to monitor the stress in the cross-section, stain gauges were employed to monitor the stress on the reinforced bars and MEMS inclinometers were used to monitor the rotation of the selected cross-sections. As the results, the M-ϕ relation can be obtained from the monitoring data. It was found that the measured moment agree well with the actual applied moment, the trend of the angle measured by inclinometer is reasonable as expected. The data of the responses obtained from the local damage monitoring can be used for the nonlinear analysis for RC structure.

KEYWORDS: *Smart aggregate, RC structure, M-ϕ, Inclinometer, Plastic hinge zone*

1. INTRODUCTION

Numerical simulation method is a good tool to evaluate the structure performance under extreme loading conditions such as earthquakes or blasts without great financial input on destruction tests. However, great difficulties still exist in accurate simulation of the nonlinear behaviour of large structures due to the uncertainty of constitutive parameter of the composed material. The measured data-based monitoring method supplied an effective way to reveal it. The globe monitoring method can be obtained by the accelerometer sensors. However, it is time-consuming and need for a detailed and accurate three-dimensional finite element model. The local monitoring method provides M-ϕ constitutive relationship by embedding sensors in the key structural position could be a feasible way.
Traditional strain gauges like fiber optic sensors and foil strain gauge, when embedded in a RC structure, cannot measure the damage process reliably under large strain cyclic loading because their bondages with the concrete tend to be loose. A commercially available load cell can measure the stress in the concrete directly, but issues such as size of the cell, its bondage with the concrete and cost may hinder its application. Many embedded-type smart sensors featuring good compatibility with concrete have been developed. For example, the cement-based piezo-resistive sensors which incorporate the conductive material (e.g. nickel, carbon black, carbon fiber, carbon nanofibers, carbon nanotubes and steel fiber) into cement paste matrix have been vastly studied (Sun et al., 2014, Teomete, 2014, Gong et al., 2011, Han et al., 2009, Han et al., 2011, Xiao et al., 2011, Xiao et al., 2010, Li et al., 2006, Wen and Chung, 2001, Galao et al., 2014), and another type of cement-based piezo-electric ceramic sensors which consist of the piezoelectric ceramic power and white cement have also been proposed (Dong et al., 2011). However, their measurement results may be significantly affected by the variation of the moisture in monitoring region due to the fact that electrical conductive of the sensor are influenced by the water molecules. A cement-based smart aggregate (SA) composed of a d33-mode lead zirconate titanate (PZT) patch sandwiched into cement mortar through water-proof material was proposed by song et al (Song et al., 2005). By evaluating the wave propagation among SAs, the damage level of the concrete structure can be detected in a qualitative manner

(Gu and Moslehy, 2010, Moslehy et al., 2010, Laskar et al., 2009, Yan et al., 2009, Song et al., 2008). The application SA has also been extended to measure the compressive stress by means of calibrating SA in relatively low stress levels (Li et al., 2006, Yang et al., 2005). To monitor the whole damage process of RC structure, the granite-based SA has been developed by Hou et al (Zhang et al., 2015, Hou et al., 2013, Hou et al., 2013, Hou et al., 2012). However, few studies have been exploded the ability of embedded-type smart sensors to monitor the RC structures.

In this study, the proposed SA was embedded in the reinforced concrete column for stress monitoring under dynamic cyclic loading. The traditional strain gauge and inclinometer was also embedded into the RC structure to monitor the M-ϕ curve. The feasibility and reasonability of the proposed method was demonstrated.

2. EXPERIMENTAL SETUP

2.1. Details of the specimen

The dimensions and reinforcement layout of the RC specimen are shown in Figure 2.1. It consists of a 238mm diameter and 1510mm long column cast integrally with a 1200mm×500mm×500mm stub. The column represents the part of a building column between the section of maximum moment and the point of contraflexure. The stub represents a discontinuity footing. Within the footing, the longitudinal reinforcing bars of the RC column were anchored with 135^{o} hooks at their ends. The column was reinforced with six 14mm-diameter longitudinal reinforcing bars and 10mm-diameter smooth stirrups, with 135^{o} hooks at both ends. The stirrups were placed with a spacing of 200mm in the assumed plastic hinge zone. The spacing of stirrups in the tested RC columns was decreased to 120mm out of the plastic hinge zone to produce higher shear resistance and prevent possible shift of shear failure. Six columns with a 152mm diameter and 305 mm height were casted with the RC specimen, and the 28-day mean compressive strength was 35.0 MPa. The deformed reinforced bars 14mm in diameter were used as the longitudinal reinforcing bars and round reinforcing bars of 10mm in diameter were used as transverse stirrups. The strength of longitudinal reinforcing bar and strirrup is 385 MPa and 450MPa, respectively.

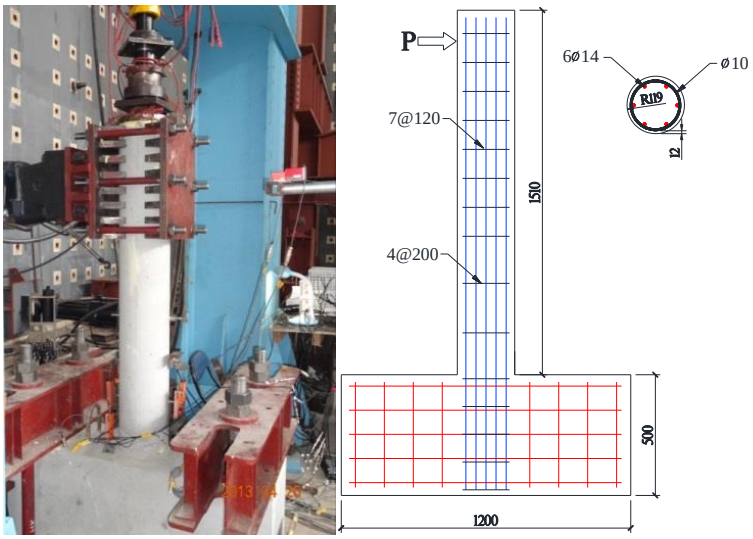

Figure 2.1 The photo of RC specimen and its reinforcing detail.

2.2. Location of the embedded sensors

The SA, strain gauge and inclinometer was embedded in the RC specimen to investigate the M-ϕ relationship of the plastic-hinge zone. The position of the embedded SA and inclinometer was shown in Figure 2.2. Six SAs were embedded in the assuming plastic hinge zone. The interval of the SAs along the height of the column is 200mm, and the spacing of the SAs along the horizontal direction is 55mm. Four stain gauges were attached on the longitudinal reinforced bars. Three inclinometers were embedded into the bottom of the specimen with the interval of 100mm along the height of the column.

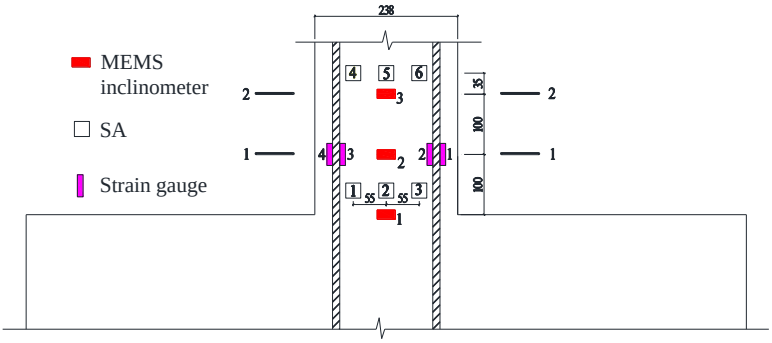

Figure 2.2 The position of embedded SA and inclinometer.

3. LOADING PROCEDURE

The lateral load was applied using a horizontally positioned 500kN MTS actuator. A load cell was fixed under the hydraulic jack to monitoring the axial load and displacement during the loading process. Displacement control manner was conducted with the amplitude of each cycle: 2, 4, 6, 8, 10, 12, 20, 30, 40, 50, and 60mm as shown in Figure 3.1. Each kind of amplitude was three cycles. The frequency is 0.5Hz. Because of the loading rate is beyond the capacity of the MTS, the last loading amplitude was only 50mm, which is less than pre-set 60mm.

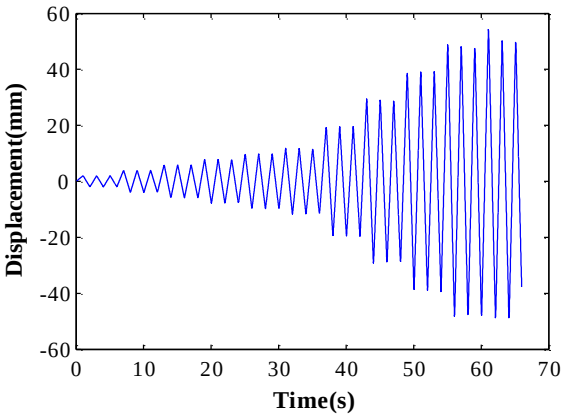

Figure 3.1 Loading procedure of displacement control.

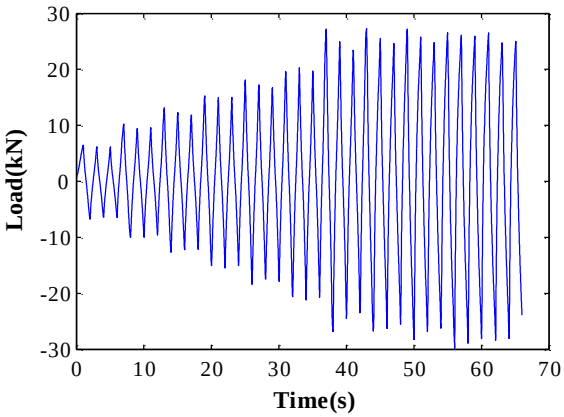

Figure 3.2 Lateral loading history.

The loading history was shown in Figure 3.2, when the loading time is beyond 38s, the load amplitude is basically a constant. It can be indicated that the reinforced bar was yield when the lateral displacement was 20mm.

4. RESULTS

As shown in Figure 4.1, the hysteretic curve is full, and it also shows the yield displacement is 20mm and strength is 27kN.

In this paper, tensile stress was defined as negative. The stresses monitored by SAs are shown in Figure 4.2, from Figure 4.2 (a), the stresses measured by SA1 increase with the loading amplitude increases, but after the reinforced bar yield, the amplitude of the stress is close to constant. The stresses measured by SA3 are about a constant, it indicates the stress of SA3 was influenced by the reinforced bar. The measured stress is larger than -1MPa indicates the tensile strength is about 1MPa. As shown in Figure 4.2 (b), the stress amplitude measured by SA4 and SA6 is basically the same, and the phase is 180^{o}, indicating the stress measured by SA4 and SA6 is reasonable. As shown in Figure 4.2 (c), the stress of the amplitude measured by SA2 and SA5 is basically the

same, the phase is 180^{o}, and the compressive amplitude is the same as tensile amplitude, which results from the position of SA2 and SA5 is in the neutral axis. The overall trend of the stress is big in the ends and small in the middle of the column cross-section, which agrees well with the theoretical stress distribution.

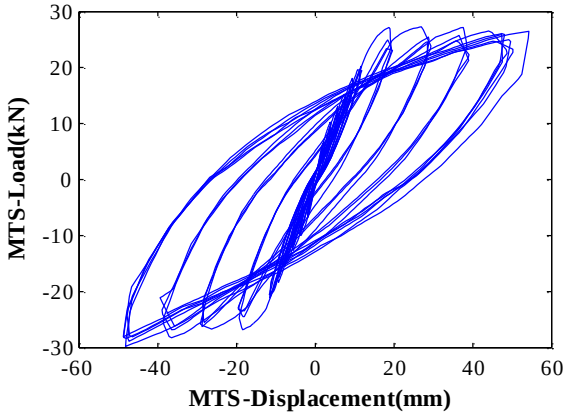

Figure 4.1 Hysteretic curve

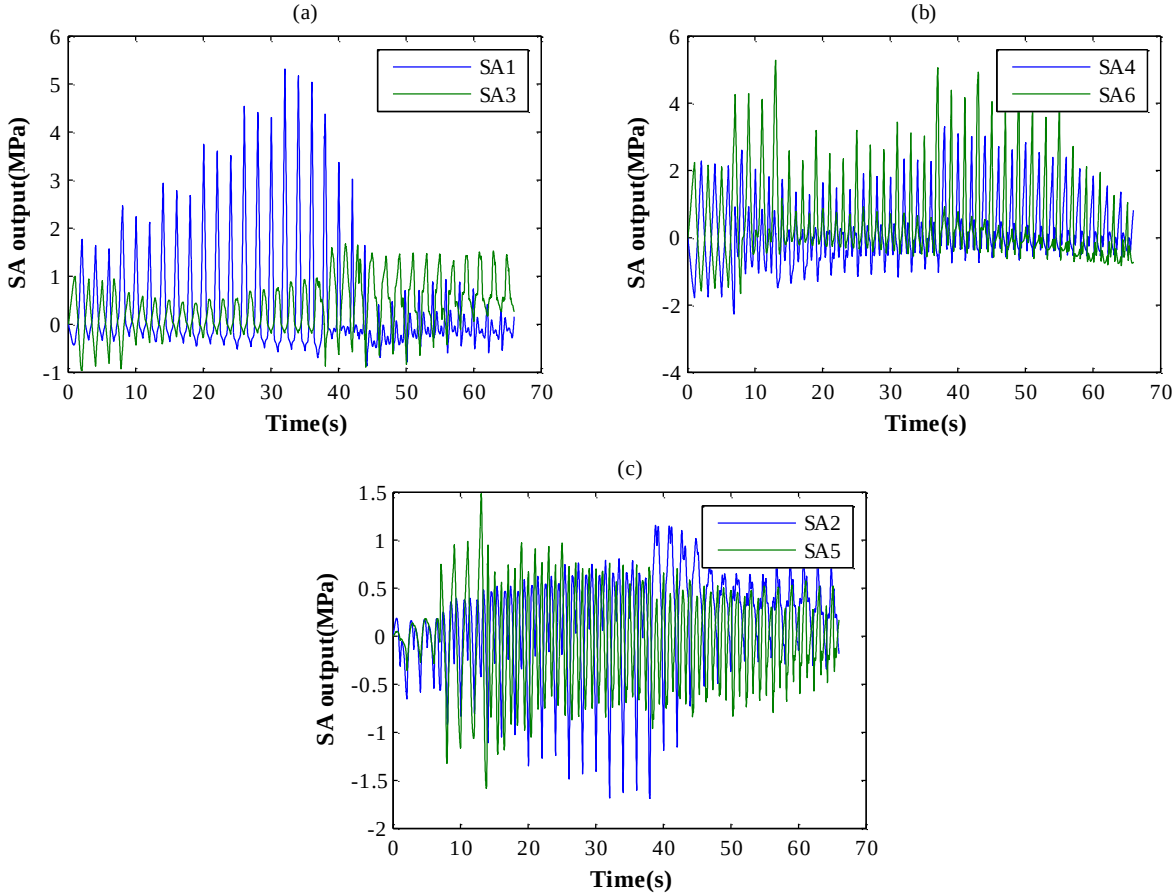

Figure 4.2 Stress measured by SAs: (a) SA1 and SA3;(b)SA4 and SA6;(c)SA2 and SA5

The strain of the reinforced bar is shown in Figure 4.3. It shows that the strain gauge 3and 4 was out of work when the reinforced bar was yield.

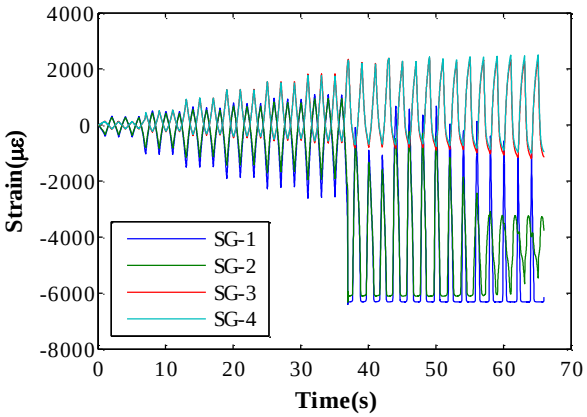

Figure 4.3 Strain of the longitudinal reinforced bar.

The moment of the section can be calculated by the following equation

$$M = \frac{\sigma I_z}{y} + \sum \varepsilon E_s A d \tag{4.1}$$

Where M is the moment of the section, σ is the stress measured by SA. I_z is the moment of inertia of cross-section. y is the distance between the centre of SA and neutral axial. E_s is the elastic modulus of the longitudinal reinforced bar. A is the area of the cross-section of longitudinal reinforced bar. d is the distance between the longitudinal reinforced bar and the neutral axial.

As shown in Figure 4.4, the moment measured by SA and strain gauge was calculated by using equation 4.1 and compared with the lateral MTS load. It can be found that the measured load is about half of the MTS-load. It is caused by the stress measured by the middle longitudinal reinforced bar was simplified to be 0.5 times of the outer longitudinal reinforced bar. Actually, when the outer longitudinal reinforced bar is yield, the stress of the middle bar will still increase. The compressive peak is basically the same. Based on the symmetry of the MTS-load, the measured load can be adjusted to fit the MTS-load. The photo of the plastic hinge zone is shown in Figure 4.5.

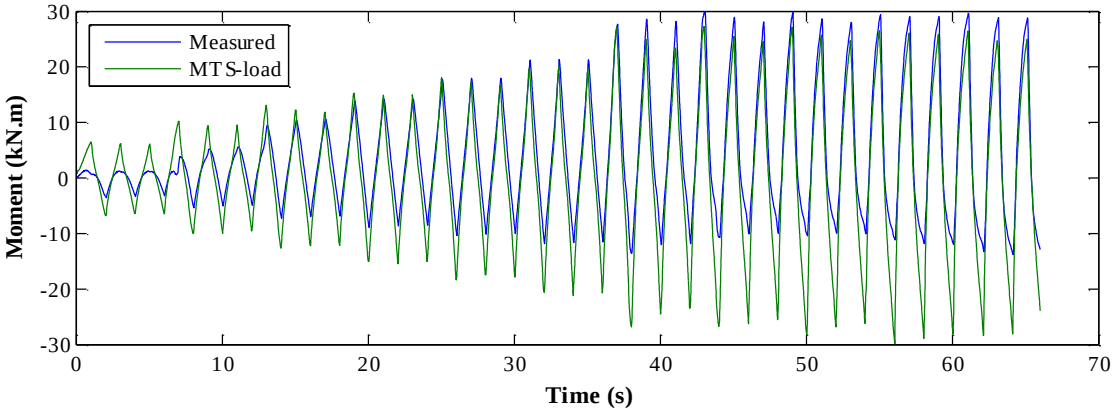

Figure 4.4 The measured moment vs time

Figure 4.5 The photo of the crack at the plastic hinge zone.

The curvature of the plastic hinge zone can be calculated by the measured rotation using following equation

$$\phi(n) = \frac{\tan(\theta_n - \theta_1)}{L} \tag{4.2}$$

Where n is 2 or 3, θ_i is the rotation measured by i^{th} inclinometer. L is the spacing of the adjacent inclinometer, which is 100mm.

As shown in Figure 4.6, the angle of the rotation measured by inclinometer increases with the height of the section and loading amplitude increases. The frequency is the same as the input load. The angle of the rotation measured by inclinometer1 indicated the rotation of the footing cannot be neglected.

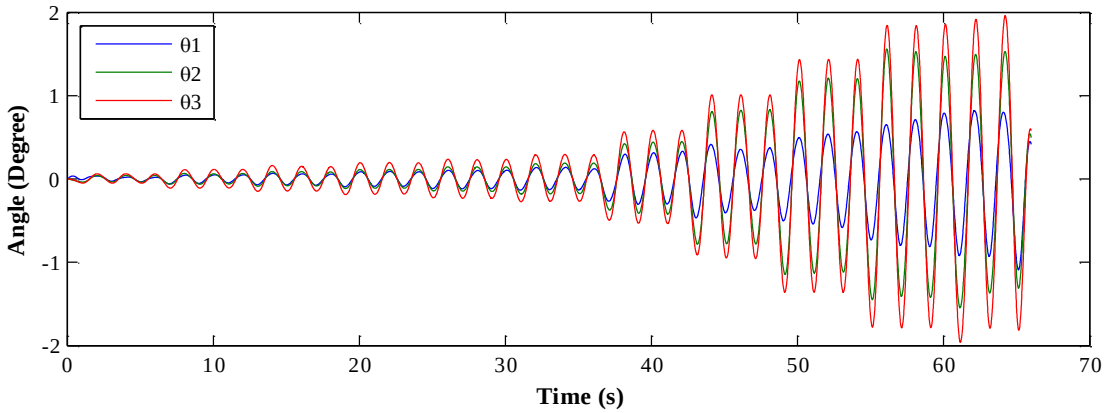

Figure 4.6 Angle of the rotation measured by inclinometers

As shown in Figure 4.7, the curvature of the plastic hinge zone was given by using the equation 4.2. The curvature of the bottom is larger than the upper zone after the reinforced bar yield. The maximum curvature is 0.01/mm.

The relationship between the measured moment and the measured curvature is shown in Figure 4.8. As expected, the curvature of section1 is larger than the section2. The curve is full and anti-symmetric.

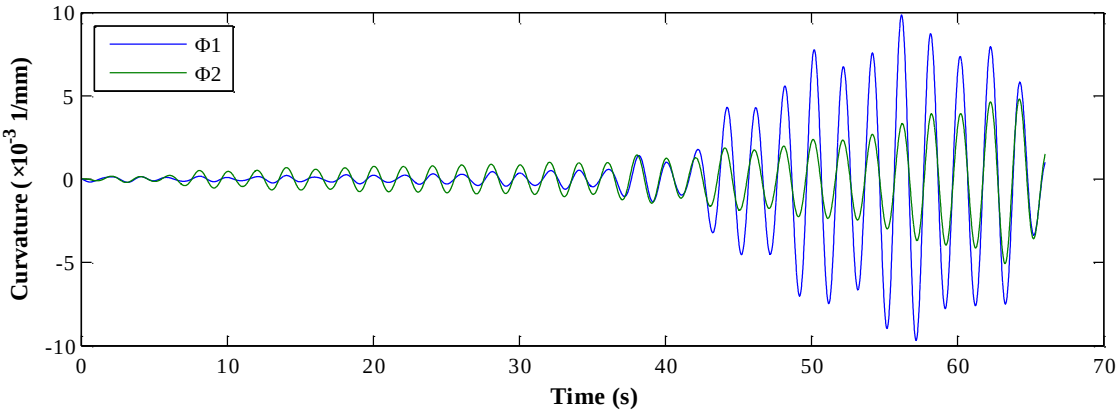

Figure 4.7 Curvature of the plastic hinge zone

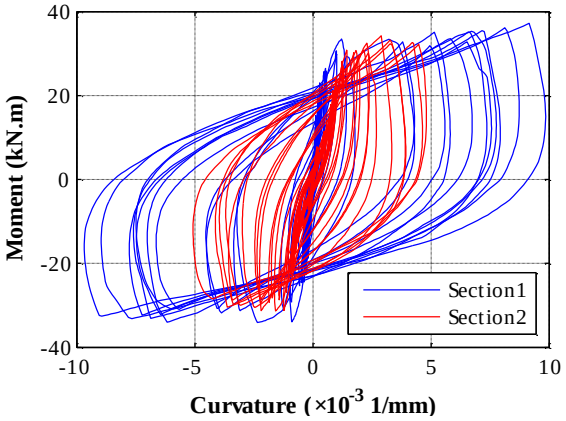

Figure 4.8 The relationship between measured moment and curvature

5. CONCLUSION

This paper proposed the M-ϕ relationship monitoring method in plastic hinge zone of the RC structure. The following conclusion can be marked.

1. The M-ϕ curve can be obtained by using SA, strain gauge and inclinometer. The amplitude of the measured moment agrees well with the applied moment, indicating the moment measured method is reasonable.
2. The angle of the rotation measured by inclinometer increases with the height and amplitude increase. The curvature decreases with the height increases as expected, implying the curvature measuring method is reasonable.

AKCNOWLEDGEMENT

Joint financial supports from the National Science Foundation of China (Grant No. 51261120376) and the National Science Foundation of China (Grant No. 91315301-12) are gratefully acknowledged.

REFERENCES

1. DONG, B., XING, F. & LI, Z. (2011). Cement-Based Piezoelectric Ceramic Composite and Its Sensor Applications in Civil Engineering. *ACI Materials Journal*, **108:5**, 543-549.
2. ELIÁŠ, J., VOŘECHOVSKÝ, M., SKOČEK, J. & BAŽANT, Z. P. (2015). Stochastic discrete meso-scale simulations of concrete fracture: Comparison to experimental data. *Engineering Fracture Mechanics*, **135:0**,

1-16.
3. GALAO, O., BAEZA, F. J., ZORNOZA, E. & GARCES, P. (2014). Strain and damage sensing properties on multifunctional cement composites with CNF admixture. *Cement and Concrete Composites*, **4690-98**.
4. GONG, H., ZHANG, Y., QUAN, J. & CHE, S. (2011). Preparation and properties of cement based piezoelectric composites modified by CNTs. *Current Applied Physics*. **11:3**, 653-656.
5. GU, H. & MOSLEHY, Y. (2010). Multi-functional smart aggregate-based structural health monitoring of circular reinforced concrete columns subjected to seismic excitations. *Smart Materials and Structures*, **19:6**, 065026.
6. HAN, B. G., HAN, B. Z. & OU, J. P. (2009). Experimental study on use of nickel powder-filled Portland cement-based composite for fabrication of piezoresistive sensors with high sensitivity. *Sensors and Actuators, A: Physical*. **149:1**, 51-55.
7. HAN, B., YU, X., ZHANG, K., KWON, E. & OU, J. (2011).Sensing properties of CNT-filled cement-based stress sensors. *Journal of Civil Structural Health Monitoring*. **1:1-2**, 17 - 24.
8. HOU, S., YU, Y., ZHANG, H. B., MAO, X. Q. & OU, J. P. (2013). A SA-Based Wireless Seismic Stress Monitoring System for Concrete Structures. *International Journal of Distributed Sensor Networks*. **2013**:**2013**
9. HOU, S., ZHANG, H. B. & OU, J. P. (2012). A PZT-based smart aggregate for compressive seismic stress monitoring. *Smart Materials and Structures*. **21:10**, 105035.
10. HOU, S., ZHANG, H. B. & OU, J. P. (2013).A PZT-based smart aggregate for seismic shear stress monitoring. *Smart Materials and Structures*. **22:6**, 065012.
11. LASKAR, A., GU, H., MO, Y. L. & SONG, G. (2009). Progressive collapse of a two-story reinforced concrete frame with embedded smart aggregates. *Smart Materials and Structures*. **18:7**.
12. LI, H., XIAO, H. & OU, J. (2006). Effect of compressive strain on electrical resistivity of carbon black-filled cement-based composites. *Cement and Concrete Composites*. **28:9**, 824 - 828.
13. LI, Z., YANG, X. & LI, Z. (2006). Application of Cement-Based Piezoelectric Sensors for Monitoring Traffic Flows. *Journal of Transportation Engineering*. **132:7**, 565-573.
14. MOSLEHY, Y., GU, H., BELARBI, A., MO, Y. L. & SONG, G. (2010). Smart aggregate based damage detection of circular RC columns under cyclic combined loading. *Smart Materials and Structures*. **19:6**.
15. RODGERS, J. E. & CELEBI, M. (2006). Seismic response and damage detection analyses of an instrumented steel moment-framed building. *Journal of Structural Engineering*. **132:10**, 1543-1552.
16. SONG, G., GU, H. & MO, Y. (2008). Smart aggregates: multi-functional sensors for concrete structures—a tutorial and a review. *Smart Materials and Structures*. **17:3**, 033001.
17. SONG, G., GU, H., MO, Y. L., HSU, T., DHONDE, H. & ZHU, R. R. H. (2005). Health monitoring of a concrete structure using piezoceramic materials. *Smart Structures and Materials 2005: Sensors and Smart Structures Technologies for Civil, Mechanical, and Aerospace Systems*. **5765:1**, 108-119.
18. SUN, M., LIEW, R. J. Y., ZHANG, M. & LI, W. (2014). Development of cement-based strain sensor for health monitoring of ultra high strength concrete. *Construction and Building Materials*, **65630-637**.
19. TEOMETE, E. (2014). Transverse strain sensitivity of steel fiber reinforced cement composites tested by compression and split tensile tests. Construction and Building Materials, **55136-145**.
20. WANG, X. F., YANG, Z. J., YATES, J. R., JIVKOV, A. P. & ZHANG, C. (2014). Monte Carlo simulations of mesoscale fracture modelling of concrete with random aggregates and pores. *Construction and Building Materials*. **7535-45**.
21. WANG, X., YANG, Z. & JIVKOV, A. P. (2015). Monte Carlo simulations of mesoscale fracture of concrete with random aggregates and pores: A size effect study. *Construction and Building Materials*, **80262-272**.
22. WEN, S. & CHUNG, D. D. L. (2001). Carbon fiber-reinforced cement as a strain-sensing coating. *Cement and Concrete Research*, **31:4**, 665-667.
23. WU, B., HUANG, X. & LU, J. (2005). Biaxial compression in carbon-fiber-reinforced mortar, sensed by electrical resistance measurement. *Cement and Concrete Research*. **35:7**, 1430-1434.
24. XIAO, H., LI, H. & OU, J. (2010). Modeling of piezoresistivity of carbon black filled cement-based composites under multi-axial strain. *Sensors and Actuators: A Physical*. **160:1-2**, 87-93.
25. XIAO, H., LI, H. & OU, J. (2011). Strain sensing properties of cement-based sensors embedded at various stress zones in a bending concrete beam. *Sensors and Actuators, A: Physical*. **167:2**, 581-587.
26. YAN, S., SUN, W., SONG, G., GU, H., HUO, L., LIU, B. & ZHANG, Y. (2009). Health monitoring of reinforced concrete shear walls using smart aggregates. *Smart Materials and Structures*. **18:4**.
27. YANG, X., LI, Z., DING, Y. & LI, Z. (2005). Test on Sensor Effect of Cement Matrix Piezoelectric Composite. *Transactions of Tianjin University*. **11:2**, 133-136.
28. ZHANG, H. B., HOU, S. & OU, J. P. (2015). SA-based seismic stress monitoring system using a specially designed charge amplifier. *Journal of Intelligent Material Systems and Structures*, under review.